Developmental Cell

Supplemental Information

Systemic Organ Wasting Induced by Localized Expression of the Secreted Insulin/IGF Antagonist *ImpL2*

Young Kwon, Wei Song, Ilia A. Droujinine, Yanhui Hu, John M. Asara, and Norbert Perrimon

Supplemental Figures

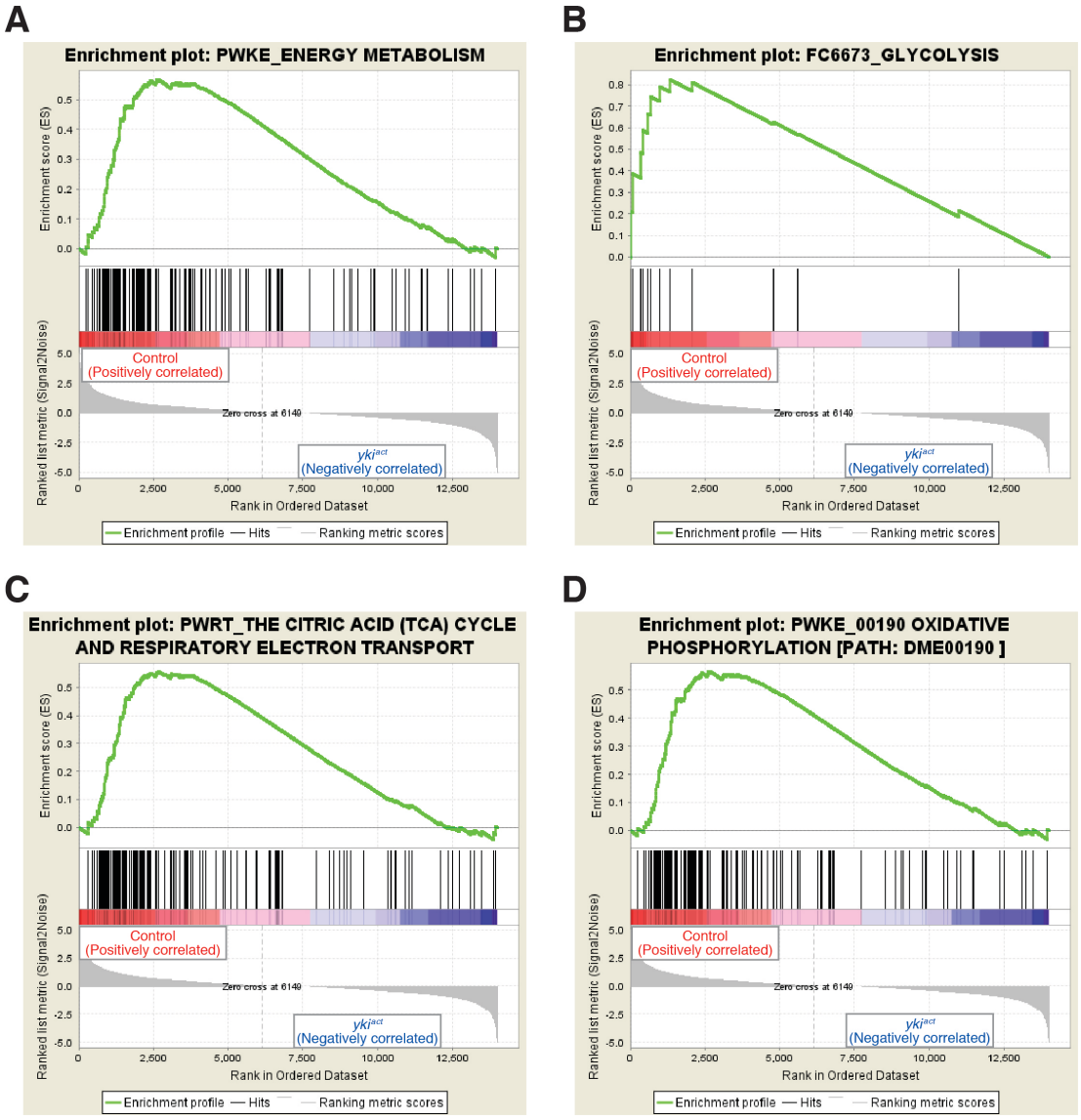

Figure S1. Representative GSEA plots showing repression of genes involved in energy metabolism in *esg^{ts}>yki^{act}* muscle transcriptome (related to Figure 2). (**A**) Energy metabolism (KEGG; normalized p value=0.000, GSEA). (**B**) Glycolysis (COMPLEAT; normalized p value=0.000, GSEA). (**C**) The citric acid (TCA) cycle and respiratory electron transport (Reactome; normalized p value=0.000, GSEA). (**C**) Oxidative phosphorylation (KEGG; normalized p value=0.000, GSEA). Additional information is shown in Table S4.

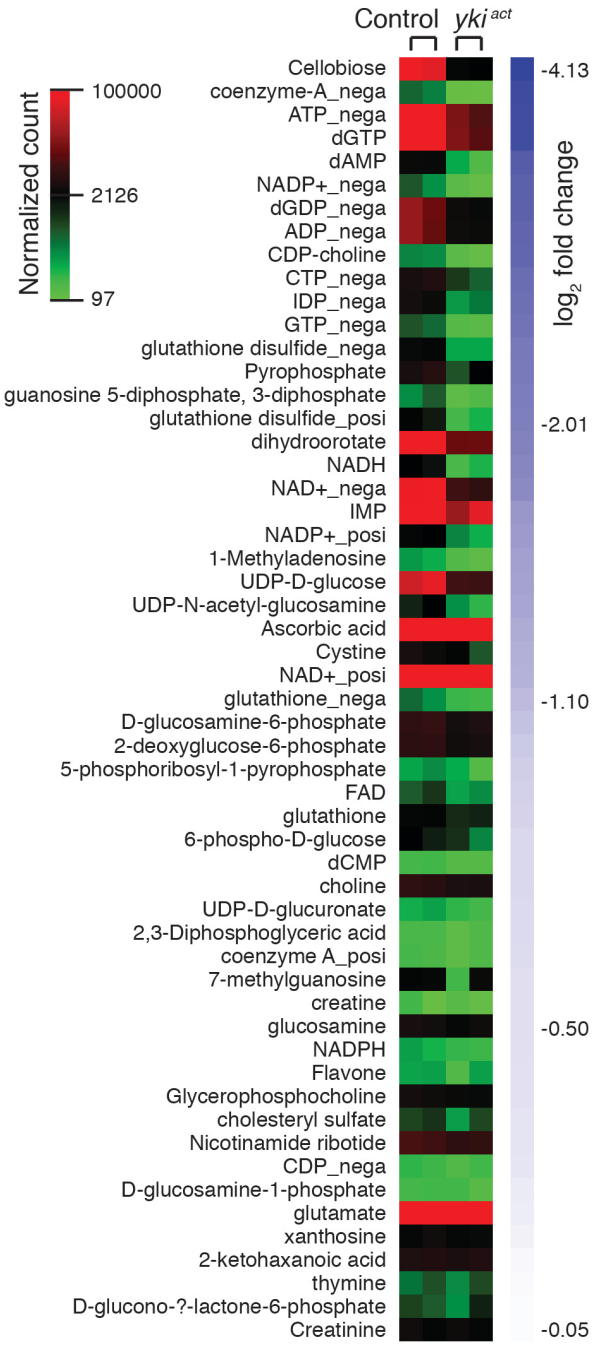

Figure S2. Reduced metabolites in hemolymph of *esg*^{ts}>*yki*^{act} flies (related to Figure 2). Heat map shows metabolite measurements of two experimental replicates of control and two experimental replicates of *esg*^{ts}>*yki*^{act}, which are normalized to the number of flies. Log_2 fold change values relative to control are indicated next to the heat map (blue bar).

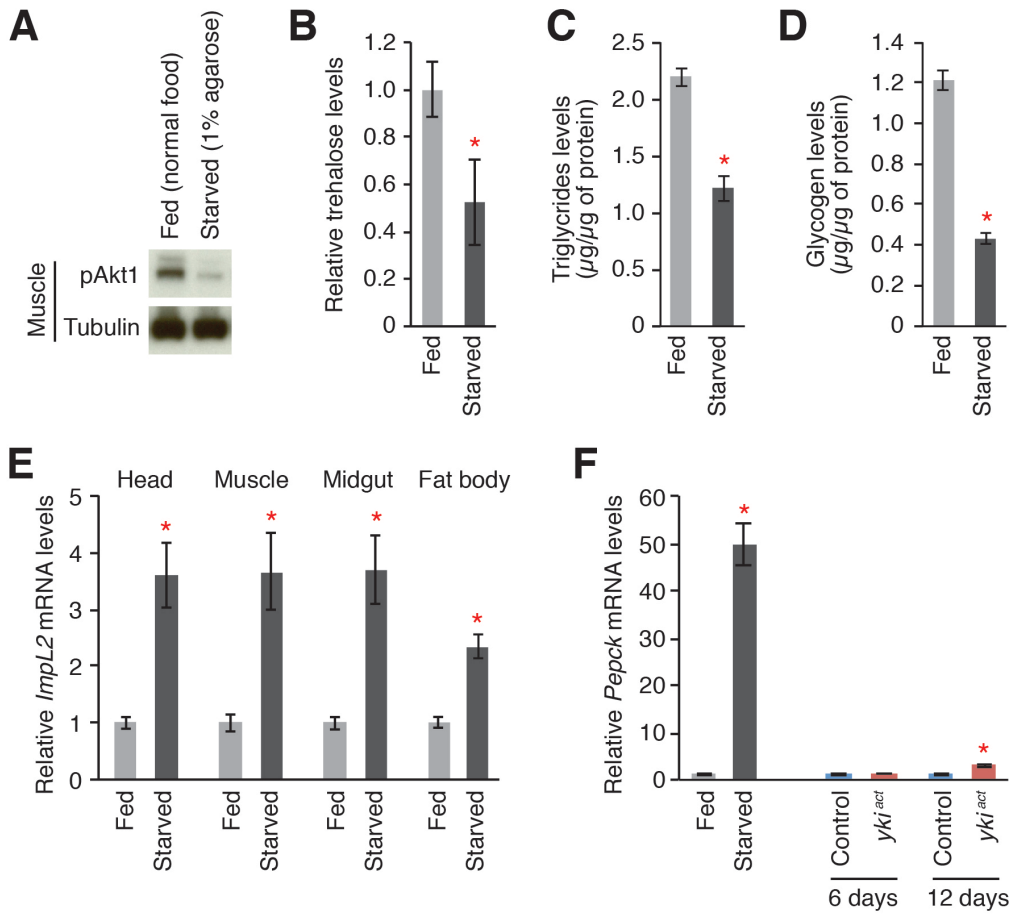

Figure S3. Characterization of starvation associated phenotypes (related to Figure 3). (**A**) Akt1 phosphorylation. (**B**) Whole body trehalose levels. Trehalose measurements are normalized to protein levels. (**C**) Whole body triglycerides levels. (**D**) Whole body glycogen levels. (**E**) Relative *ImpL2* mRNA expression. Relative values to controls are presented. (**F**) Relative *Pepck* mRNA expression. Genotypes of control is *esg-GAL4*, *tub-GAL80^{ts}*, *UAS-GFP*/+ and *yki^{act}* is *esg-GAL4*, *tub-GAL80^{ts}*, *UAS-GFP/+; UAS-yki^{act}/+*. Controls were fed on either normal food (Fed) or 1% agarose (Starved) for 24 hours. All measurements shown are mean±SDs. *p≤0.05 (Student's *t*-test) compared to control.

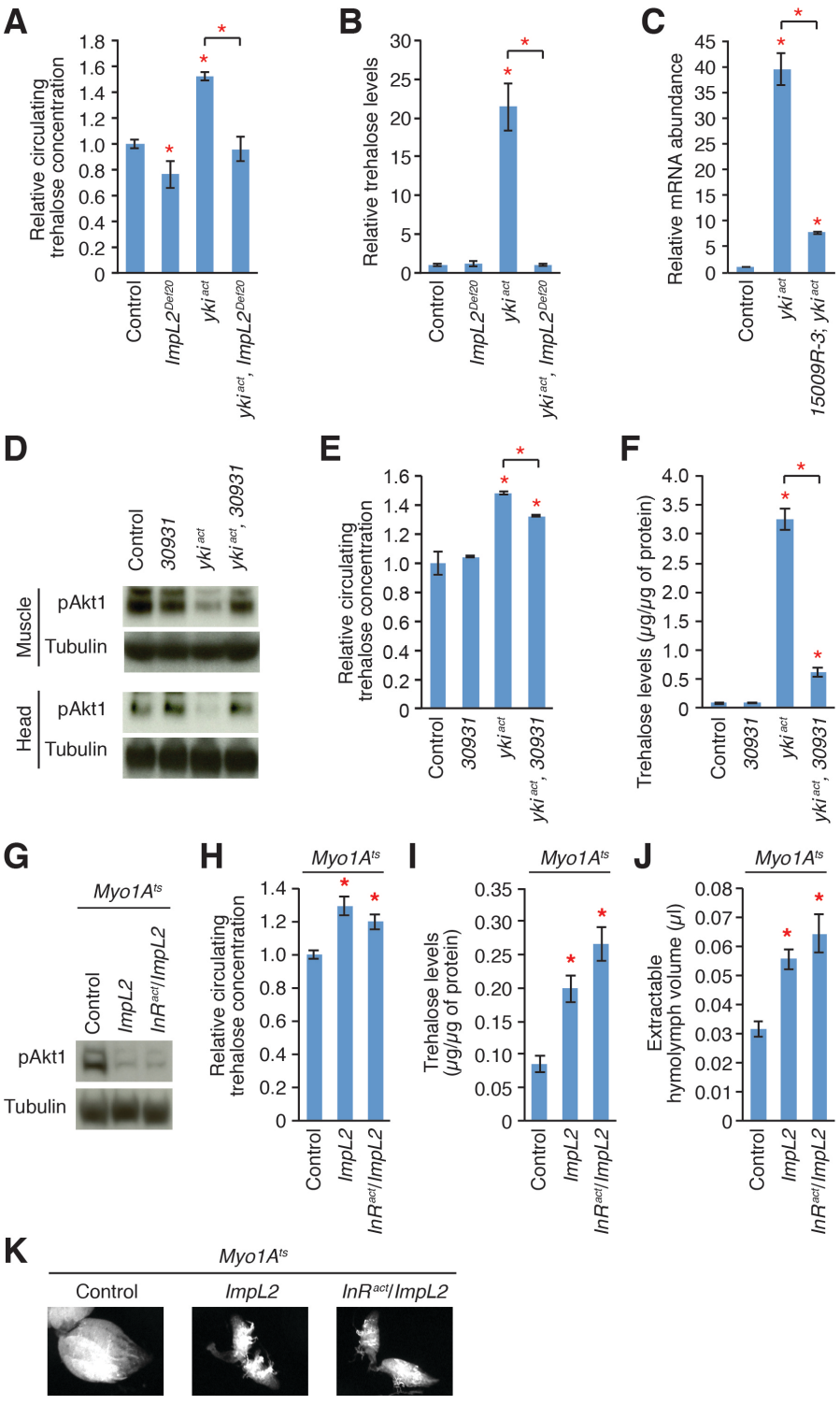

Figure S4. Further characterization of the role of ImpL2 (related to Figure 4). (**A-B**) Rescue of hyperglycemia associated with *esg*^{ts}>*yki*^{act} by *ImpL2*^{Def20}. Transgenes are induced with *esg*^{ts}. (**A**) Circulating trehalose concentrations at 8 days of induction. (**B**)

Relative trehalose levels in whole-body at 8 days of induction. Trehalose measurements are normalized to total protein amounts. (**C**) Relative expression levels of *ImpL2* in the midgut following expression of an *ImpL2*-RNAi line, *15009R-3* (NIG) with esg^{ts}. Expression levels are measured by qPCR. Values shown are mean±SDs. (**D-F**) Rescue of hyperglycemia and reduction of insulin/IGF signaling associated with $esg^{ts}>yki^{act}$ by depletion of *ImpL2* with an additional *ImpL2*-RNAi line, *30931*. Transgenes are induced with esg^{ts}. (**D**) Akt1 phosphorylation (pAkt1) in muscle and head at 8 days of induction. (**E**) Circulating trehalose concentrations at 8 days of induction. (**F**) Trehalose levels in whole-body at 8 days of induction. Measurements are normalized to total protein amounts. *30931* is an RNAi line against *ImpL2* obtained from VDRC. Genotypes in (**A-F**) are as follows: control is *esg-GAL4*, $tub\text{-}GAL80^{ts}$, *UAS-GFP*/+, yki^{act} is *esg-GAL4*, $tub\text{-}GAL80^{ts}$, *UAS-GFP*/+; $UAS\text{-}yki^{act}$/+, *30931* is *esg-GAL4*, $tub\text{-}GAL80^{ts}$, *UAS-GFP*/+; *30931*/+, yki^{act}, *30931* is *esg-GAL4*, $tub\text{-}GAL80^{ts}$, *UAS-GFP*/+; *30931,* $UAS\text{-}yki^{act}$/+, and other genotypes are as shown in Figure 4. (**G-K**) Systemic phenotypes induced by ectopic expression of *ImpL2* in midgut enterocytes. Transgenes are induced with $tub\text{-}Gal80^{ts}$; *Myo1A-GAL4*, *UAS-GFP* ($Myo1A^{ts}$) by shifting to 29°C. To avoid a direct effect on enterocytes caused by overexpression of *ImpL2*, we also combined an active form of the *Insulin-like receptor* (InR^{act}) (Wittwer et al., 2005), whose expression provides a cell-autonomous protection from the action of *ImpL2*. (**G**) Akt1 phosphorylation in muscle. Expression of *ImpL2* with or without InR^{act} decreased Akt1 phosphorylation in muscles. (**H**) Circulating trehalose concentrations. (**I**) Trehalose levels in whole-body. (**J**) Hemolymph volumes extractable from whole-flies. (**K**) Images of ovary at 8 days of induction. Overexpression of either *ImpL2* alone or together with an active form of *InR* (InR^{act}) in enterocytes causes ovary atrophy. All metabolic assay results shown are mean±SEMs. *p≤0.05 (Student's *t*-test) compared to control unless indicated with a bracket.

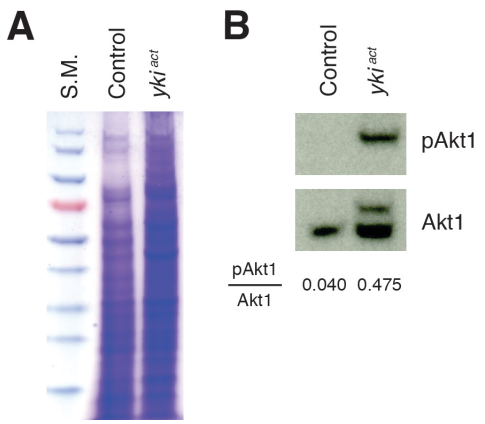

Figure S5. Measurement of Akt1 phosphorylation in the midgut (related to Figure 6). (A) Coomassie staining of the protein extracts from midgut. Protein extracts of five midguts from each genotype were run on SDS-PAGE gel, then stained with Coomassie brilliant blue. (**B**) Detection of phospho-Akt1 (pAkt1) and Akt1 by western blotting. Transgenes are induced with *esg*^{ts} for 6 days. Genotypes of control is *esg-GAL4*, *tub-GAL80*^{ts}, *UAS-GFP*/+ and *yki*^{act} is *esg-GAL4*, *tub-GAL80*^{ts}, *UAS-GFP*/+*; UAS-yki*^{act}/+.

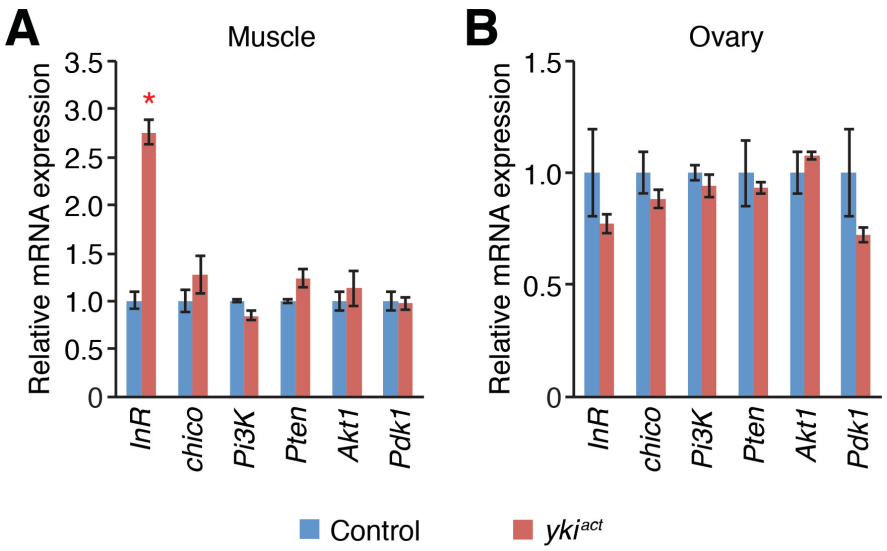

Figure S6. Relative mRNA abundance of insulin/IGF pathway components in muscle (A) and ovary (B) (related to Figure 6). Transgenes were induced for 6 days with *esg*^{ts}. Values shown are mean±SDs. *p<0.05, unpaired Student's *t*-test.

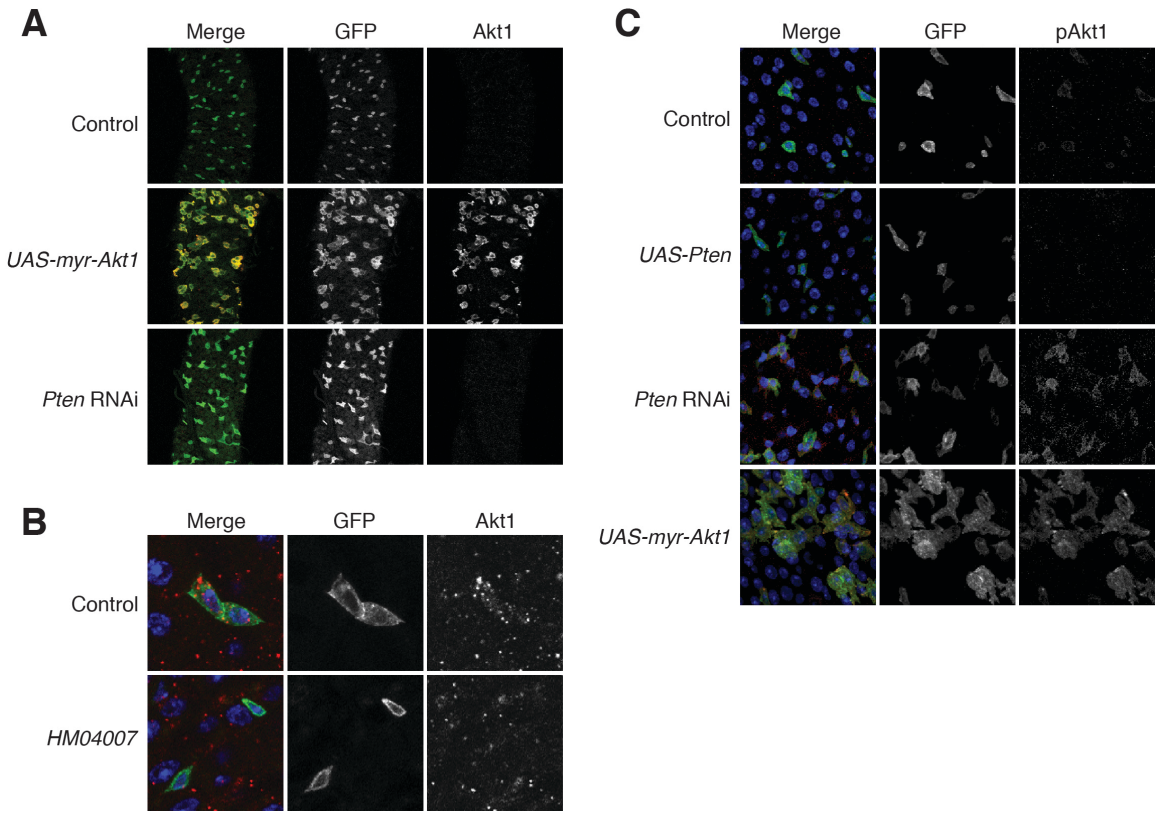

Figure S7. Characterization of anti-Akt and anti-phospho-*Drosophila* Akt antibodies in the midgut (related to Figure 6). (**A**) Detection of Akt1. Overexpression of myr-Akt1, but not activation of Akt1 by knockdown of *Pten*, specifically enhanced the fluorescent signal detected with the anti-Akt antibody (red in merge). GFP (green in merge) marks the midgut progenitor cells. Transgenes were induced for 6 days. (**B**) Detection of Akt1. Knockdown of *Akt1* with the RNAi line *HM04007* (TRiP) reduced basal Akt1 signal (red in merge) in the stem cells (GFP; green in merge). Akt1 signal is slightly enriched in stem cells (upper panels). Transgenes were induced for 6 days. (**C**) Detection of phospho-Akt1 (pAkt1; red in merge). Overexpression of *Pten* decreased pAkt1 signal, but knockdown of *Pten* or overexpression of *myr-Akt1* increased pAkt1 signal. Transgenes were induced with esg^{ts} for 10 days.

Supplemental Tables

Table S1. Muscle RNA-Seq results (related to Figure 2). Normalized values are shown.

Table S2. Gene list enrichment analysis of the muscle transcriptome of *esg^{ts}>yki^{act}* flies (related to Figure 2). (**A**) List of downregulated genes. (**B**) List of upregulated genes. (**C**) Selected gene sets enriched in downregulated transcriptome. (**D**) Selected gene sets enriched in upregulated transcriptome.

Table S3. Network of metabolic processes enriched in the downregulated muscle transcriptome of *esg^{ts}>yki^{act}* flies (related to Figure 2). The network is shown in Figure 2A.

Table S4. GSEA results of energy metabolism (related to Figure 2). A few selected pathways involved in energy metabolism are analyzed with GSEA program (Broad Institute) (Subramanian et al., 2005).

Table S5. Metabolomics of hemolymph metabolites (related to Figure 2). Normalized values to fly number (**A**) and hemolymph volume (**B**) are shown.

Supplemental Experimental Procedures

Immunostaining of the midgut

Prior to dissection, flies were fed on 4% sucrose for ~4 hours to remove food from the midgut. Midguts were dissected in PBS and stained overnight with anti-Akt antibody (Cell Signaling Technology, 9272; 1:200) or anti-phospho *Drosophila* Akt (Ser505, correspond to Ser473 in human) antibody (Cell Signaling Technology, 4054; 1:200) in PBS with 0.1% BSA, 0.3% Triton X-100 and 5% Normal Donkey Serum. Stainings were visualized with Alexa Fluor® 594 Donkey anti-rabbit IgG (Life Technologies). Maximum projections of 4-6 stacks of images across an epithelial layer were taken with a Leica TCS SP2-AOBS confocal microscope. We characterized the anti-Akt and anti-phospho-*Drosophila* Akt (Ser505) antibodies in the midgut since they were not previously used to stain Akt1 and pAkt1 in this tissue (Figure S7).

Additionally, we detected Akt1 or pAkt1 in the midgut by Western blot using the same antibodies. To inhibit proteases and phosphatases in the midgut, we homogenized 20 midguts directly in 2XSDS-PAGE sample buffer supplemented with 2 mM Benzamidine, 1 μM Pepsistatin, 1 mM PMSF, Protease inhibitor cocktail (Sigma) and Phosphatase inhibitor cocktail 1, 2 (Sigma). We ran the protein extracts corresponding to 5 midguts on SDS-PAGE. We tested protein amounts by Coomassie brilliant blue staining.

Quantification of mRNA expression

Total RNA was extracted from 15 midguts, 10 heads, 6 thoraces or 8 ovaries using TRIzol® reagent (Invitrogen, 15596-026). We synthesized first strand cDNA with 1 μg of total RNA using iScript™ Reverse Transcription Supermix (BIO-RAD, 170-8841) and performed quantitative PCR with CFX96 Real-Time System (BIO-RAD) using iQ™ SYBR Green Supermix (BIO-RAD, 170-8882). All expression values were normalized to *RpL32* (also known as *rp49*). All assays were performed in triplicate, and representative results are shown. The primer sequences used for quantitative PCR are as follows:
ImpL2, AAGAGCCGTGGACCTGGTA, TTGGTGAACTTGAGCCAGTCG;
InR, AAGCGTGGGAAAATTAAGATGGA, GGCTGTCAACTGCTTCTACTG;

chico, GCGCACTCACCTTATGACCA, GCACACGAATGTCAGGGATTT;
Pi3K, AGCCCAAGTATGAGACACCG, AACAGGCAGATTAGGTCCACC;
Pten, TCAGAAACCGTCTGGAAGATGT, CGCTCCGAGCATAGGTTATAGA;
Akt1, CCCAGCGTTACATCGGGTC, GCTCGCCCCTCTTCATCAG;
Pdk1, GTTCCCGGCTTCGTAAACCT, GCGGTTGATGTATGGCAACA;
th, GCTGGACTGGCTGGATAAAC, GCCGCAGAAAAAGCATTTAACT;
Hex-A, CTGCTTCTAACGGACGAACAG, GCCTTGGGATGTGTATCCTTGG;
Hex-C, GCGGAGGTGCGAGAACTTAT, CCACTTCCAGGCAAAAGCGA;
Pfk, CGAGCCTGTGTCCGTATGG, AGTTGGCTTCCTGGATGCAG;
Ald, GCCCAGAAAATCGTTGCCC, GGGTCAGTGCTGAACAACAG;
GAPDH, CCAATGTCTCCGTTGTGGA, TCGGTGTAGCCCAGGATT;
Eno, CGATCAAGGCCCGTCAAATCT, CCAGGGTGTCGTTCACATGG;
Pyk, GCAGGAGCTGATACCCAACTG, CGTGCGATCCGTGAGAGAA;
ImpL3, CAGCACGGCTCCAACTTTCT, GATGATGTTCTTGAGGATGTCGG;
Dilp2, ATGAGCAAGCCTTTGTCCTTC, ACCTCGTTGAGCTTTTCACTG;
Dilp3, ATGGGCATCGAGATGAGGTG, CGTTGAAGCCATACACACAGAG;
Dilp5, CGCTCCGTGATCCCAGTTC, AGGCAACCCTCAGCATGTC;
RpL32, GCTAAGCTGTCGCACAAATG, GTTCGATCCGTAACCGATGT;
Pepck, GAACTGACGGACTCTGCTTAC, GGTGCGTTCGGGATCACAA.

CAFE Assay

The CAFE assay was performed as previously described (Demontis and Perrimon, 2010; Ja et al., 2007). Briefly, 5 female flies deprived from food for 6 hours were provided with liquid food (5% yeast and 10% sucrose) maintained in 10 μl calibrated glass micropipettes. The amount of liquid food consumed was measured after incubating 10 hours.

Blue dye excretion assay

To measure food excretion rate, we fed flies with fresh food containing 2.5% (w/v) blue food dye (F D & C Blue Dye no. 1) overnight. Then, we divided the flies into two groups. One group of flies (Group A) was kept at -20°C, and the other group of flies

(Group B) was transferred onto normal food without dye. After incubating for 4 hours, flies were homogenized in 200 μl PBS. The amount of blue dye in supernatant was measured using a spectrophotometer. We calculated food excretion rate by {(blue dye amount from Group A) – (blue dye amount from Group B)} / (blue dye amount from Group A).

Dilp2 immunostaining

Dissected adults brains were fixed for 15 minutes in 4% formaldehyde. After fixation, the brains were stained overnight at 4°C with anti-dILP2 antibody (gift from Dr. Linda Partridge, University College London; 1:5000) in PBS with 0.1% BSA, 0.3% Triton X-100 and 5% Normal Donkey serum. Alexa Fluor® 594 Donkey anti-rabbit IgG (Life Technologies) was used to detect the staining. Confocal images were obtained using a Leica TCS SP2 AOBS system.

Measuring enzymatic activities in muscle

Hexokinase and Pyruvate Kinase activities in adult *Drosophila* muscle were measured using Hexokinase Colorimetric Assay Kit (Sigma-Aldrich, MAK091) and Pyruvate Kinase Activity Assay Kit (Sigma-Aldrich, MAK072) following manufacturer's protocols. Briefly, 6 thoraces were homogenized in 100 μl Hexokinase assay buffer or Pyruvate kinase assay buffer provided with the kits. After centrifugation at 14,000 rpm for 15 min at 4°C, supernatants were collected. The collected lysates were diluted 1:10 for Hexokinase assay and 1:100 for Pyruvate Kinase assay, and then 10 μl of diluted lysates were mixed with 50 μl Reaction Mixture. The measured values (Vmax) were normalized to lysate protein levels.

ATP measurement in thorax

6 thoraces were homogenized in 100 μl extraction buffer (6 M Guanidine Chloride, 100 mM Tris-HCl pH8.0, 4 mM EDTA), heated at 70°C for 5 minutes, then centrifuged at 14,000 rpm for 10 minutes at 4°C to remove cuticle and cell debris. ATP levels were measured using ATP Determination Kit (Invitrogen, A22066) following the

manufacturer's protocol and normalized to protein levels.

Electron Microscopy

We fixed thoraces in 0.1 M sodium cacodylate buffer (pH 7.4) containing 2.5% glutaraldehyde, 2% paraformaldehyde for overnight. The fixed samples were washed in 0.1M cacodylate buffer, fixed again with 1% osmiumtetroxide (OsO_4) and 1.5% potassium ferrocyanide ($KFeCN_6$) for 1 hour, and washed 3 times in water. Then, the samples were incubated in 1% aqueous uranyl acetate for 1 hour and followed by 2 washes in water and subsequent dehydration in grades of alcohol. The samples were then put in propyleneoxide for 1 hour and embedded in TAAB Epon (Marivac Canada Inc.).

Ultrathin sections (about 60nm) were cut on a Reichert Ultracut-S microtome, picked up on to copper grids, and then stained with lead citrate. The sections were examined in a JEOL 1200EX Transmission electron microscope, and images were recorded with an AMT 2k CCD camera.

Gene list enrichment analysis

For each gene, we calculated 4 combinatorial fold-change values relative to control using the DESeq normalized expression values for each gene from two control muscles and two $esg^{ts}>yki^{act}$ muscles RNA-Seq results. We selected genes as differentially expressed genes (upregulated or downregulated genes) if at least 3 out of these 4 combinatorial absolute $\log_2$ fold-change values were 1 or higher. Consequently, we identified 645 upregulated genes (4.6% of entire transcriptome) and 749 downregulated genes (5.3% of entire transcriptome) in the $esg^{ts}>yki^{act}$ muscles compared to control muscles (Table S1 and S2).

For gene list enrichment analysis, we first assembled gene lists, including pathways, complexes and target gene sets of transcription factors, from various public resources such as Gene Ontology (http://www.geneontology.org/), KEGG (Ogata et al., 1999), BioCarta (http://www.biocarta.com/), FlyReactome (http://fly.reactome.org/), DroID (Murali et al., 2011), COMPLEAT (Vinayagam et al., 2013) and Reactome (Croft et al., 2014). The gene lists from other species were converted into *Drosophila* gene lists

using an orthologous mapping tool DIOPT (Hu et al., 2011) with the least stringent filter setup. We performed enrichment analysis with up- and down-regulated muscle transcriptomes separately. Enrichment p values of gene lists were calculated using hyper-geometric distribution, and selected gene lists with p value less than 0.05 were presented (Table S2). Additionally, we analyzed a few selected metabolic pathways using GSEA program (Subramanian et al., 2005) (http://www.broadinstitute.org/gsea/index.jsp).

Supplemental References

Croft, D., Mundo, A.F., Haw, R., Milacic, M., Weiser, J., Wu, G., Caudy, M., Garapati, P., Gillespie, M., Kamdar, M.R.*, et al.* (2014). The Reactome pathway knowledgebase. Nucleic Acids Res *42*, D472-477.

Demontis, F., and Perrimon, N. (2010). FOXO/4E-BP signaling in Drosophila muscles regulates organism-wide proteostasis during aging. Cell *143*, 813-825.

Hu, Y., Flockhart, I., Vinayagam, A., Bergwitz, C., Berger, B., Perrimon, N., and Mohr, S.E. (2011). An integrative approach to ortholog prediction for disease-focused and other functional studies. BMC Bioinformatics *12*, 357.

Ja, W.W., Carvalho, G.B., Mak, E.M., de la Rosa, N.N., Fang, A.Y., Liong, J.C., Brummel, T., and Benzer, S. (2007). Prandiology of Drosophila and the CAFE assay. Proc Natl Acad Sci U S A *104*, 8253-8256.

Murali, T., Pacifico, S., Yu, J., Guest, S., Roberts, G.G., 3rd, and Finley, R.L., Jr. (2011). DroID 2011: a comprehensive, integrated resource for protein, transcription factor, RNA and gene interactions for Drosophila. Nucleic Acids Res *39*, D736-743.

Ogata, H., Goto, S., Sato, K., Fujibuchi, W., Bono, H., and Kanehisa, M. (1999). KEGG: Kyoto Encyclopedia of Genes and Genomes. Nucleic Acids Res *27*, 29-34.

Subramanian, A., Tamayo, P., Mootha, V.K., Mukherjee, S., Ebert, B.L., Gillette, M.A., Paulovich, A., Pomeroy, S.L., Golub, T.R., Lander, E.S.*, et al.* (2005). Gene set enrichment analysis: a knowledge-based approach for interpreting genome-wide expression profiles. Proc Natl Acad Sci U S A *102*, 15545-15550.

Vinayagam, A., Hu, Y., Kulkarni, M., Roesel, C., Sopko, R., Mohr, S.E., and Perrimon, N. (2013). Protein complex-based analysis framework for high-throughput data sets. Sci Signal *6*, rs5.

Wittwer, F., Jaquenoud, M., Brogiolo, W., Zarske, M., Wustemann, P., Fernandez, R., Stocker, H., Wymann, M.P., and Hafen, E. (2005). Susi, a negative regulator of Drosophila PI3-kinase. Dev Cell *8*, 817-827.